JACS
JOURNAL OF THE AMERICAN CHEMICAL SOCIETY
Article
pubs.acs.org/JACS

Direct Observation of Photodissociation Products from Phenylperoxyl Radicals Isolated in the Gas Phase

Alan T. Maccarone,[†] Benjamin B. Kirk,[†] Christopher S. Hansen,[†] Thomas M. Griffiths,[†] Seth Olsen,[‡] Adam J. Trevitt,*[,†] and Stephen J. Blanksby*[,†]

[†]ARC Centre of Excellence for Free Radical Chemistry and Biotechnology, School of Chemistry, University of Wollongong, NSW 2522, Australia

[‡]School of Physics, University of Queensland, QLD 4072, Australia

Supporting Information

ABSTRACT: Gas phase peroxyl radicals are central to our chemical understanding of combustion and atmospheric processes and are typically characterized by strong absorption in the UV ($\lambda_{max} \approx 240$ nm). The analogous maximum absorption feature for arylperoxyl radicals is predicted to shift to the visible but has not previously been characterized nor have any photoproducts arising from this transition been identified. Here we describe the controlled synthesis and isolation *in vacuo* of an array of charge-substituted phenylperoxyl radicals at room temperature, including the 4-(*N*,*N*,*N*-trimethylammonium)methyl phenylperoxyl radical cation (4-$Me_3N^{[+]}CH_2-C_6H_4OO^{\bullet}$), using linear ion-trap mass spectrometry. Photodissociation mass spectra obtained at wavelengths ranging from 310 to 500 nm reveal two major photoproduct channels corresponding to homolysis of aryl-OO and arylO-O bonds resulting in loss of O_2 and O, respectively. Combining the photodissociation yields across this spectral window produces a broad (FWHM ≈ 60 nm) but clearly resolved feature centered at λ_{max} = 403 nm (3.08 eV). The influence of the charge-tag identity and its proximity to the radical site are investigated and demonstrate no effect on the identity of the two dominant photoproduct channels. Electronic structure calculations have located the vertical $\tilde{B} \leftarrow \tilde{X}$ transition of these substituted phenylperoxyl radicals within the experimental uncertainty and further predict the analogous transition for unsubstituted phenylperoxyl radical ($C_6H_5OO^{\bullet}$) to be 457 nm (2.71 eV), nearly 45 nm shorter than previous estimates and in good agreement with recent computational values.

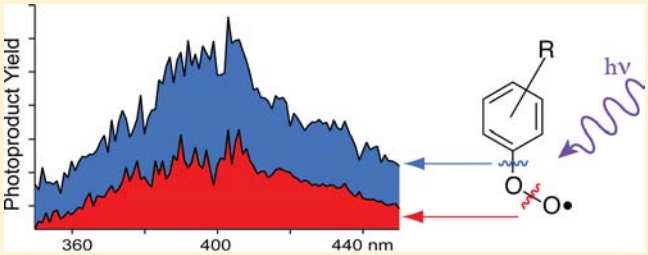

INTRODUCTION

Organic peroxyl radicals play an important role in many fundamental processes, including cellular lipid oxidation and DNA damage,[1,2] decomposition of fuels in combustion,[3,4] and oxidation of volatile organic compounds in the atmosphere.[5−8] The intrinsic gas-phase chemistry of alkylperoxyls is increasingly understood, with key kinetic, thermodynamic and spectroscopic properties elucidated from both computation and experiment.[9−13] In contrast, there exists a paucity of direct observations of arylperoxyl radicals to validate their intermediacy in gas-phase chemical models including those describing soot formation,[14−16] combustion,[17−21] and tropospheric processing of hydrocarbons.[22−26] The importance of arylperoxyls in understanding these chemistries is emphasized by the high proportion of aromatic components in contemporary petroleum fuels, with allowances of up to 45% in some countries.[27,28]

In the vast majority of cases, the formation and fate of peroxyl radicals in gas-phase laboratory experiments has been established using time-resolved UV spectroscopy.[24,29] Innumerable measurements have identified the characteristic absorption of alkylperoxyl radicals between 210 and 300 nm (e.g., $CH_3OO^{\bullet}$ λ_{max} = 237 nm, 5.23 eV, FWHM ∼60 nm)[29] corresponding to vertical excitation to the dissociative $\tilde{B}$ state.[12,29,30] This work has been complemented by characterization of near-IR transitions to the bound, low-lying $\tilde{A}$ states of peroxyl radicals (e.g., $CH_3OO^{\bullet}$ T_{00} = 1354.5 nm, 0.92 eV).[31,32] Miller and co-workers used this transition to characterize gas phase phenylperoxyl radicals formed following photolysis of acetophenone in the presence of dioxygen.[33] Observations of sharp, characteristic features in the near-IR provided the first unequivocal evidence for an arylperoxyl radical in the gas phase and showed that the location of the $\tilde{A} \leftarrow \tilde{X}$ origin transition (i.e., $C_6H_5OO^{\bullet}$ T_{00} = 1334 nm, 0.93 eV) is not significantly perturbed by the presence of the aryl moiety. In contrast, computational predictions of the energy of the $\tilde{B}$ state of the phenylperoxyl radical predict a significant red-shift compared with alkylperoxyl radicals with estimates of λ_{max} ranging from 337 to 503 nm.[11,12,34,35] Indeed two groups have reported monitoring a putative $\tilde{B} \leftarrow \tilde{X}$ transition near 500 nm at room temperature to establish second order rate constants for the addition of dioxygen to the phenyl radical but in neither instance was a major absorption feature clearly resolved.[36,37]

Received: March 21, 2013
Published: May 23, 2013

More recently, Freel et al. reported resolved vibronic bands attributed to the jet-cooled phenylperoxyl radical.[38] The $\tilde{B} \leftarrow \tilde{X}$ band origin was assigned at 570.84 nm (T_{00} = 2.17 eV) and vibronic assignments were made to a number of features out to ca. 513 nm. The measured peak widths are consistent with a dissociative $\tilde{B}$ state for this radical with overall spectral broadening suggesting that room temperature absorption spectra may be broad and featureless. In this context, we have deployed photodissociation action spectroscopy to characterize the $\tilde{B} \leftarrow \tilde{X}$ transition of substituted phenylperoxyl radicals at room temperature and provide the first identification of photoproducts arising from this dissociative electronic state.

Gas phase spectroscopy of reactive radicals must balance the sometimes competing demands of maximizing the number density of the target species while minimizing undesired self-reactions and reducing background absorption. Installing a fixed charge moiety ("charge-tag") within the molecule, but remote from a radical center, (i) allows straightforward purification of products in a reaction mixture using standard mass spectrometry techniques and (ii) eliminates self-reaction of targeted radicals by virtue of their mutual repulsion. As such, carefully selected radical ions have proved useful for extracting relative reaction rates,[39] efficiencies[40] and products[41] from which the behavior of the corresponding neutral could be inferred. Here we apply this approach in a photodissociation (PD) action spectroscopy experiment on charge-substituted phenylperoxyl radicals (e.g., 4-$Me_3N^{[+]}CH_2-C_6H_4OO^{\bullet}$) synthesized and isolated in the gas phase inside a modified linear ion-trap mass spectrometer.[42]

METHODS

Experimental Section. *Para*-iodoaniline was purchased from Sigma-Aldrich (Castle Hill, NSW, Australia) and the three salts *N*-(4-iodobenzyl)-*N*,*N*,*N*-trimethylammonium iodide, 4-iodo-*N*,*N*,*N*-trimethylbenzenaminium iodide, and 3-iodo-*N*,*N*,*N*-trimethylbenzenaminium iodide were synthesized according to the method reported by Kirk et al.[40] Each salt was dissolved in HPLC grade methanol (Ajax Finechem, Sydney, NSW, Australia) to a final concentration of 50 μM for direct infusion at 5 μL/min through the electrospray ionization (ESI) source of a Thermo Fisher Scientific (San Jose, CA) LTQ linear ion-trap mass spectrometer. Typically the spray needle voltage was set to 4 kV, the tube lens voltage to 80 V and the capillary voltage at 20 V. The heated capillary temperature was maintained at 100 °C and nitrogen was used for the sheath, auxiliary and sweep gases. This ion-trap mass spectrometer has previously been structurally modified to enable irradiation of an ion population during trapping with either fixed frequency or tunable laser sources.[42,43] Here we implement a software modification which allows synchronization between (i) one laser system and a given isolation step of the ion trap and (ii) a second laser system and another isolation step in the same MS^n sequence. Comprehensive details of this synchronization and the hardware involved are given as Supporting Information. All mass spectra shown below are an average of 40−50 scans.

Computational. All calculations reported here were performed using the Gaussian 09 suite of codes.[44] Density Functional Theory (DFT) was employed to optimize all ground state geometries using either BLYP/6-31G(d) or B3LYP/6-311+G(d) functional/basis set.[45] Time Dependent DFT (TDDFT) was chosen to locate the excited state energy levels with either BLYP/6-31+G(d) or M06/6-311++G(d,p).[46] Concise tabulations of the pertinent results are provided as Supporting Information.

RESULTS AND DISCUSSION

Scheme 1 depicts the experimental procedure whereby precursor cations of *m*/*z* 276 (**2**) are generated by electrospray ionization (ESI) of a suitable salt (**1**) and mass-selected in a quadrupole linear ion-trap mass spectrometer. Following isolation, one pulse at 266 nm (4.66 eV) from a Nd:YAG laser irradiates the ions to drive facile C−I bond cleavage[47] and generate a charge-substituted phenyl radical of *m*/*z* 149 (**3**) as the major photoproduct (see Figure S5 in Supporting Information). Isolation and subsequent trapping of **3** for 800 ms allows for reaction with background dioxygen to form the desired phenylperoxyl radicals at *m*/*z* 181 (**4**) as previously described.[40] The nascent peroxyl radical is rapidly thermalized to the temperature of the ion trap (ca. 310 K) by collisions with the helium buffer gas (present at 2.5 mTorr).[48] The peroxyl radicals **4** are then isolated for irradiation from one laser pulse of an optical parametric oscillator (OPO) at wavelengths between 310 and 500 nm (ca. 2.5−4.0 eV), and ionic photoproducts are mass analyzed.

Scheme 1. Experimental Procedure Outlining the Gas-phase Synthesis, Isolation, and Photodissociation of Substituted Phenylperoxyl Radicals

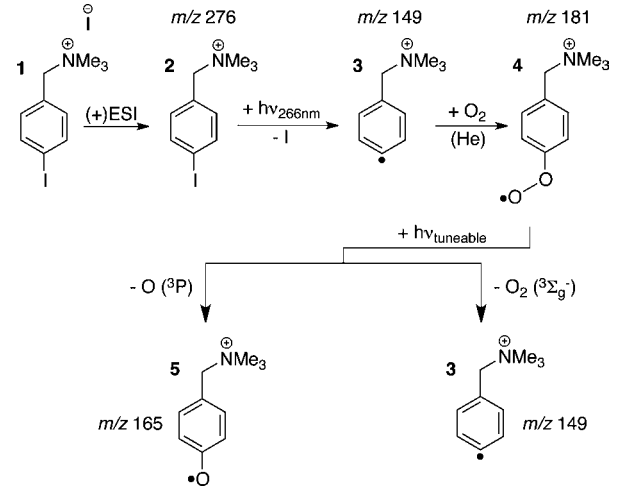

Representative mass spectra of the charge-tagged peroxyl radical **4** at selected photodissociation wavelengths are shown in Figure 1. These data show that the major photoproducts in all cases appear at *m*/*z* 149 and 165 corresponding to the substituted phenyl radical **3** (with neutral loss of O_2) and substituted phenoxyl radical **5** (via loss of O), respectively. Calculations at the B3LYP/6-311+G(d) level of theory yield 40.0 and 39.3 kcal mol^{-1} for homolysis of the C−OO and the CO−O bonds, respectively, and indicate that both channels are energetically accessible at wavelengths less than ca. 730 nm (1.70 eV). Together these two channels account for at least 95% of the total product flux from the photodissociation of **4**, with less than 5% attributable to other products unrelated to the photochemistry of the arylperoxyl moiety (e.g., *m*/*z* 59 $Me_3N^{\bullet[+]}$ is observed but not shown in Figure 1). To our knowledge, this is the first direct experimental identification of photoproducts from a phenylperoxyl radical in the gas phase.

The data in Figure 1 also suggest an absorption profile peaking between 390 and 440 nm. To further examine this, averaged mass spectra were collected at 1 nm steps between 350 and 450 nm and the results are plotted in Figure 2 as power corrected PD action spectra (defined in the Supporting Information). A broad absorption profile for **4** can be inferred from the total photoproduct yield (black dots in Figure 2). Prior UV spectra of peroxyl radicals at ambient temperatures have been well described by a Gaussian distribution.[29,30]

dx.doi.org/10.1021/ja402610s | J. Am. Chem. Soc. 2013, 135, 9010−9014

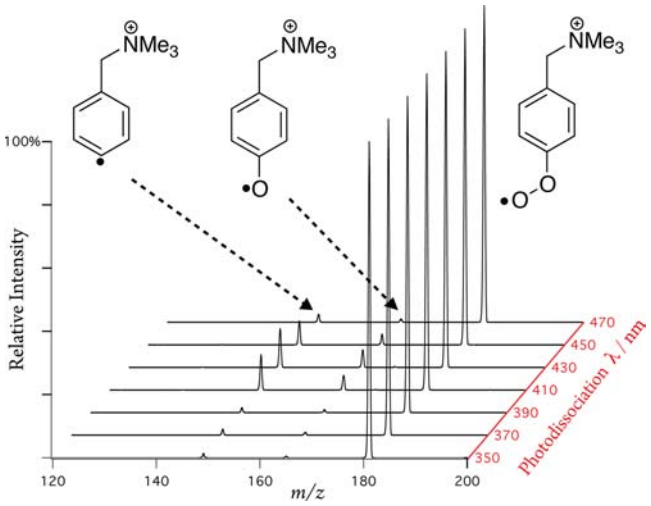

Figure 1. Mass spectra resulting from the photodissociation of the substituted phenylperoxyl radical **4** (m/z 181) obtained at representative wavelengths between 350 and 470 nm. Ion abundance in each spectrum is normalized to m/z 181.

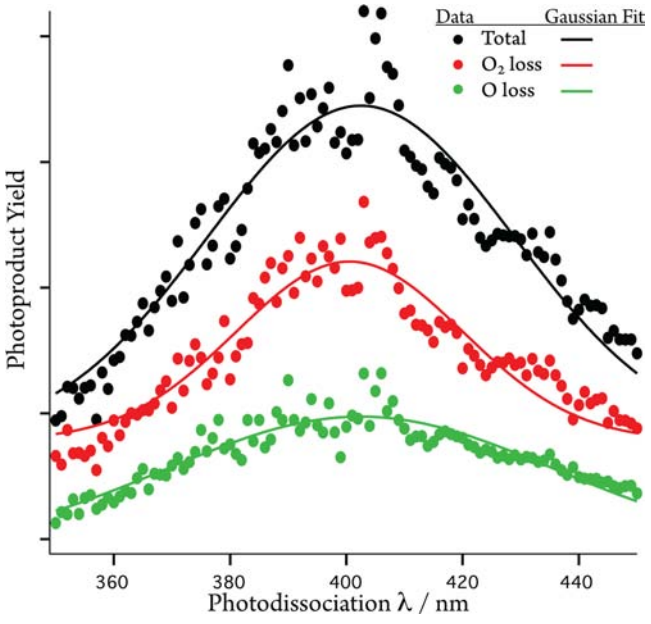

Figure 2. PD action spectra recorded from irradiating **4** over the indicated OPO wavelength region.

Applying this fit here yields a λ_{max} at 403 nm (3.08 eV) with a full width at half-maximum (FWHM) around 60 nm (0.46 eV). The data from Figure 2 can also be analyzed to show that nearly 60% of the relative photoproduct flux at 403 nm is accounted for by O_2 loss, with ca. 40% going to atomic oxygen production.

To examine the effect of the remote charge-tag on the spectroscopy of the arylperoxyl radical, we collected PD action spectra for each of three analogues **6**, **7** and **8** (structures shown in Table 1, spectra in Figure S2 of the Supporting Information). Table 1 summarizes the results showing λ_{max} from fitted values for each radical ion in the far right column. Within the experimental uncertainty of these assignments, the identity of the charge carrier causes a small (less than 10 nm) shift of the absorption maximum (e.g., trimethyl ammonium cation for **6** compared to an ammonium cation for **8**). Attaching the charge

Table 1. Vertical $\tilde{B} \leftarrow \tilde{X}$ Transition Energies from Experiment and Theory for the Phenylperoxyl Radical and Substituted Analogues Studied Herein

Molecule	Method	Reference	Energy / nm
	Room Temp. Cavity Ring-Down	36&37	495 - 531
	TDDFT:BLYP/6-31+G(d)	35	503
	CAS/DZd-ROHF	34	337
	TDDFT: B3LYP/aug-cc-pVTZ	38	441
	TDDFT:M06/6-311++G(d,p)	this work	457
4 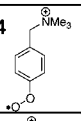	PD Action Spectroscopy	this work	403 ± 10[a]
	TDDFT:M06/6-311++G(d,p)	this work	411
6 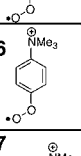	PD Action Spectroscopy	this work	393 ± 9
	TDDFT:M06/6-311++G(d,p)	this work	394
7 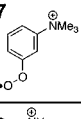	PD Action Spectroscopy	this work	403 ± 5
	TDDFT:M06/6-311++G(d,p)	this work	398
8 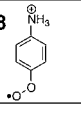	PD Action Spectroscopy	this work	386 ± 5
	TDDFT:M06/6-311++G(d,p)	this work	383

[a]Errors reported as ±1 std. dev. of avg. from at least 2 data sets.

carrier directly to the aromatic ring at the *para*-position gave rise to a small but reproducible blue-shift (ca. 10 nm between **4** and **6**), while installing the same moiety at the *meta*-position moved the λ_{max} back to the red (cf. **6** and **7**). Importantly, only the photodissociation channels producing atomic and molecular oxygen were observed for **6**–**8**; no signal at m/z 59 was observed for **6** and **7**. Both of these results strengthen the claim that the peroxyl radical moiety overwhelmingly determines the photodissociation dynamics in this suite of substituted arylperoxyls.

While small changes in the relative position of the charged and radical moieties do not significantly impact the absorption profile, the presence of the charge may be expected to shift the absorption maximum relative to the neutral phenylperoxyl. This can be rationalized using the general valence bond (GVB) orbital representations drawn in Figure 3.[49] The ground state of

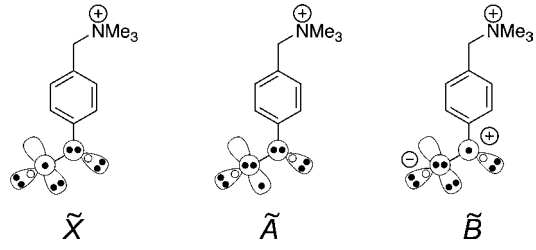

Figure 3. GVB diagrams of the lowest three electronic states for the arylperoxyl radical **4**.

the radical cation **4** may be stabilized by delocalization of an electron pair onto the ring, while conversely the $\tilde{B}$ state appears perturbed to higher energy due to a formal positive charge on the ring-bonded oxygen, viz. net electron density movement away from the $Me_3N^{[+]}$ charge-tag. Indeed, comparing the experimental values obtained here with the two reported room temperature spectra for the neutral phenylperoxyl vertical absorption band (Table 1)[36,37] suggests that the charge may be responsible for a blue shift as large as ca. 100 nm. To investigate

dx.doi.org/10.1021/ja402610s | J. Am. Chem. Soc. 2013, 135, 9010–9014

this we have computed the vertical excitation energies for the homologous series 4-$Me_3N^{[+]}(CH_2)_n$-$C_6H_4OO^{\bullet}$, where n = 0−6, using time-dependent density functional theory (TDDFT). These results (see Supporting Information, Figure S6) show a decrease in the vertical $\tilde{B} \leftarrow \tilde{X}$ transition energy as n increases, producing a trend toward 460 nm for n = 6 which is approximately equal to the value calculated for the neutral phenylperoxyl radical (*vide infra*) at the same level of theory. These data demonstrate that, the presence and the proximity of the charge in our experimental systems is responsible for a shift in the maximum absorption feature of some 60 nm to the blue. Nevertheless, our experimental data provide a robust training set for theoretical predictions of vertical $\tilde{B} \leftarrow \tilde{X}$ transitions in gas-phase arylperoxyls radicals.

TDDFT was also used to predict the observed vertical $\tilde{B} \leftarrow \tilde{X}$ transition energies for the substituted and the neutral phenylperoxyl radicals. A detailed description of these computations is provided as Supporting Information and the results, along with predictions from literature reports using different computational methods and basis sets, are shown in Table 1. The BLYP functional was employed by Weisman and Head-Gordon with the 6-31+G(d) basis set to yield a value of 503 nm for the neutral in good agreement with the experimental work of Yu and Lin.[35,36] We applied the same functional and basis set to each of the substituted phenylperoxyl radicals from this study and found the vertical $\tilde{B} \leftarrow \tilde{X}$ transition wavelengths red-shifted ∼60 nm from our experimental values (e.g., **4** in Table S1 of Supporting Information). TDDFT computations performed in our study with a larger basis set and the robust M06 functional predict the experimental transition energies within the associated uncertainty for each of the substituted phenylperoxyl radicals examined here.[50] Accordingly, applying this functional and basis set to compute the $\tilde{B}$ state energy level for neutral phenylperoxyl yielded a value of 457 nm. This estimate is 45 nm blue-shifted from the experimental value of Yu and Lin[36] but not as far as the 337 nm computed by Krauss and Osman.[34] Freel et al. also employed TDDFT and found the B3LYP functional with the aug-cc-pVTZ basis performed well when benchmarked to their experimental origin band energy.[38] Using this method, they reported a vertical $\tilde{B} \leftarrow \tilde{X}$ transition of 441 nm, in good agreement with our calculations.

CONCLUSIONS

Taken together, the experimental and computational results reported here (Table 1) suggest that the commonly reported λ_{max} for the vertical $\tilde{B} \leftarrow \tilde{X}$ transition in neutral arylperoxyl radicals of ca. 500 nm may need to be re-evaluated; our results suggests this feature lies closer to 457 nm (2.71 eV). Correct spectral assignment of the $\tilde{B} \leftarrow \tilde{X}$ transition in room temperature arylperoxyl radicals is critical for validation of their intermediacy in gas-phase hydrocarbon oxidation and measurement of robust reaction kinetics. For example, several groups have monitored a putative phenylperoxyl absorption at ca. 500 nm in order to derive the rate constants for the fundamental reaction of phenyl radical and dioxygen.[36,37] Our findings suggest that only the low energy tail of the phenylperoxyl absorption is monitored near 500 nm or indeed the time-resolved behavior of this feature might belong to an alternate intermediate or isomer. The former of these two ideas is supported by a recently reported jet-cooled $C_6H_5OO^{\bullet}$ absorption spectrum.[38] The authors posit that broadened features will frustrate attempts to record a room temperature phenylperoxyl absorption spectrum with any distinguishing features near 500 nm. Hence it seems visible wavelength strategies for detection of gas-phase arylperoxyl radicals under ambient conditions are perhaps best suited to photoproduct analysis techniques, for example, action spectroscopy.

Finally, it is intriguing to consider the implications of these findings for understanding the photochemical fate of arylperoxyl radicals formed in the atmosphere. Jafri and coworkers proposed that the dissociative $\tilde{B} \leftarrow \tilde{X}$ state of alkylperoxyl radicals could give rise to $O(^3P)$ that upon addition to O_2 would provide a pathway for ozone (O_3) formation that was independent of the well-known NO_x cycle.[51,52] The consequences of this proposal have not been widely considered because (i) the dissociative $\tilde{B} \leftarrow \tilde{X}$ transition for alkylperoxyl radicals falls outside the actinic spectrum while (ii) the photoproducts of arylperoxyl radicals were hitherto unknown. Here we demonstrate for the first time that photoactivation of arylperoxyl radicals in the visible yields ground state atomic oxygen and may therefore contribute to daytime ozone concentrations in the troposphere. The results also suggest that any substituted monocyclic arylperoxyl, for example, oxidized xylenes from petroleum fuels, could exhibit similar photochemistry upon absorption at visible wavelengths. And although polycyclic arylperoxyls originating from sources such as edge-oxidized soot particles are expected to absorb at longer visible wavelengths with increasing size (greater π network for resonance stabilization of the $\tilde{B}$ state),[15,53] their photoproducts should remain dominated by O and O_2 loss. These ideas advocate for a reassessment of the mechanisms via which arylperoxyls might influence atmospheric chemistry.

ASSOCIATED CONTENT

Supporting Information

Detailed experimental methods; PD mass and action spectra for radicals **6**, **7**, and **8**; and PD mass spectra for precursor **2** and the three analogous iodinated compounds used as precursors for **6**, **7**, and **8**. Optimized ground state geometries with corresponding energies (in Hartrees) from computations are also listed along with results from excited state energy calculations for each radical. This material is available free of charge via the Internet at http://pubs.acs.org.

AUTHOR INFORMATION

Corresponding Author

blanksby@uow.edu.au; adamt@uow.edu.au

Notes

The authors declare no competing financial interest.

ACKNOWLEDGMENTS

We are grateful to Dr. Jae C. Schwartz from Thermo Fisher Scientific (San Jose, CA) for providing a software patch which allows synchronization of the LTQ ion-trap mass spectrometer activation sequencing with each of the two separate lasers used in our experiments (see Supporting Information for more details). We thank Dr. Gabriel da Silva and Prof. Leo Radom for helpful discussions and Mr. Bradley Speed (UOW) for results obtained from related compounds. S.J.B. and A.J.T. acknowledge the financial support of UOW and the Australian Research Council through its Centre's of Excellence (CE0561607) and Discovery Programs (DP0986738).

REFERENCES

(1) Krumoya, K.; Friedland, S.; Cosa, G. *J. Am. Chem. Soc.* **2012**, *134*, 10102.
(2) Hong, I. S.; Carter, K. N.; Sato, K.; Greenberg, M. M. *J. Am. Chem. Soc.* **2007**, *129*, 4089.
(3) Benson, S. W. *J. Am. Chem. Soc.* **1965**, *87*, 972.
(4) Zador, J.; Taatjes, C. A.; Fernandes, R. X. *Prog. Energy Combust. Sci.* **2011**, *37*, 371.
(5) Lelieveld, J.; Butler, T. M.; Crowley, J. N.; Dillon, T. J.; Fischer, H.; Ganzeveld, L.; Harder, H.; Lawrence, M. G.; Martinez, M.; Taraborrelli, D.; Williams, J. *Nature* **2008**, *452*, 737.
(6) Glowacki, D. R.; Lockhart, J.; Blitz, M. A.; Klippenstein, S. J.; Pilling, M. J.; Robertson, S. H.; Seakins, P. W. *Science* **2012**, *337*, 1066.
(7) Hofzumahaus, A.; Rohrer, F.; Lu, K.; Bohn, B.; Brauers, T.; Chang, C.-C.; Fuchs, H.; Holland, F.; Kita, K.; Kondo, Y.; Li, X.; Lou, S.; Shao, M.; Zeng, L.; Wahner, A.; Zhang, Y. *Science* **2009**, *324*, 1702.
(8) Paulot, F.; Crounse, J. D.; Kjaergaard, H. G.; Kuerten, A., St; Clair, J. M.; Seinfeld, J. H.; Wennberg, P. O. *Science* **2009**, *325*, 730.
(9) Xu, W.; Lu, G. *J. Phys. Chem. A* **2008**, *112*, 6999.
(10) Boyd, S. L.; Boyd, R. J.; Barclay, L. R. C. *J. Am. Chem. Soc.* **1990**, *112*, 5724.
(11) Wallington, T. J.; Dagaut, P.; Kurylo, M. J. *Chem. Rev.* **1992**, *92*, 667.
(12) Tyndall, G. S.; Cox, R. A.; Granier, C.; Lesclaux, R.; Moortgat, G. K.; Pilling, M. J.; Ravishankara, A. R.; Wallington, T. J. *J. Geophys. Res.—Atm.* **2001**, *106*, 12157.
(13) Orlando, J. J.; Tyndall, G. S. *Chem. Soc. Rev.* **2012**, *41*, 6294.
(14) Frenklach, M. *Phys. Chem. Chem. Phys.* **2002**, *4*, 2028.
(15) Raj, A.; da Silva, G. R.; Chung, S. H. *Combust. Flame* **2012**, *159*, 3423.
(16) Celnik, M. S.; Sander, M.; Raj, A.; West, R. H.; Kraft, M. *Proc. Combust. Inst.* **2009**, *32*, 639.
(17) Carpenter, B. K. *J. Am. Chem. Soc.* **1993**, *115*, 9806.
(18) Fadden, M. J.; Barckholtz, C.; Hadad, C. M. *J. Phys. Chem. A* **2000**, *104*, 3004.
(19) Tokmakov, I. V.; Kim, G. S.; Kislov, V. V.; Mebel, A. M.; Lin, M. C. *J. Phys. Chem. A* **2005**, *109*, 6114.
(20) da Silva, G.; Chen, C.-C.; Bozzelli, J. W. *J. Phys. Chem. A* **2007**, *111*, 8663.
(21) Metcalfe, W. K.; Dooley, S.; Dryer, F. L. *Energy Fuels* **2011**, *25*, 4915.
(22) Calvert, J. G.; Atkinson, R.; Becker, K. H.; Kamens, R. M.; Seinfeld, J. H.; Wallington, T. J.; Yarwood, G. *The Mechanisms of Atmospheric Oxidation of Aromatic Hydrocarbons*; Oxford University Press: New York, 2002.
(23) Jenkin, M. E.; Saunders, S. M.; Wagner, V.; Pilling, M. J. *Atm. Chem. Phys.* **2003**, *3*, 181.
(24) Cox, R. A. *Chem. Soc. Rev.* **2012**, *41*, 6231.
(25) Caralp, F.; Foucher, V.; Lesclaux, R.; Wallington, T. J.; Hurley, M. D. *Phys. Chem. Chem. Phys.* **1999**, *1*, 3509.
(26) Glowacki, D. R.; Wang, L.; Pilling, M. J. *J. Phys. Chem. A* **2009**, *113*, 5385.
(27) http://www.environment.gov.au/atmosphere/fuelquality/standards/petrol.html
(28) Battin-Leclerc, F. *Prog. Energy Combust. Sci.* **2008**, *34*, 440.
(29) Nielsen, O. J.; Wallington, T. J. In *The Chemistry of Free Radicals: Peroxyl Radicals*; Alfassi, Z. B., Ed.; Jacaranda Wiley Ltd.: Brisbane, 1997; p 69.
(30) Lightfoot, P. D.; Cox, R. A.; Crowley, J. N.; Destriau, M.; Hayman, G. D.; Jenkin, M. E.; Moortgat, G. K.; Zabel, F. *Atm. Env. A* **1992**, *26*, 1805.
(31) Pushkarsky, M. B.; Zalyubovsky, S. J.; Miller, T. A. *J. Chem. Phys.* **2000**, *112*, 10695.
(32) Miller, T. A. *Mol. Phys.* **2006**, *104*, 2581.
(33) Just, G. M. P.; Sharp, E. N.; Zalyubovsky, S. J.; Miller, T. A. *Chem. Phys. Lett.* **2006**, *417*, 378.
(34) Krauss, M.; Osman, R. *J. Phys. Chem.* **1995**, *99*, 11387.
(35) Weisman, J. L.; Head-Gordon, M. *J. Am. Chem. Soc.* **2001**, *123*, 11686.
(36) Yu, T.; Lin, M. C. *J. Am. Chem. Soc.* **1994**, *116*, 9571.
(37) Tanaka, K.; Ando, M.; Sakamoto, Y.; Tonokura, K. *Int. J. Chem. Kinet.* **2012**, *44*, 41.
(38) Freel, K.; Sullivan, M. N.; Park, J.; Lin, M. C.; Heaven, M. C. *J. Phys. Chem. A* **2013**, DOI: 10.1021/jp401570q.
(39) Amegayibor, F. S.; Nash, J. J.; Lee, A. S.; Thoen, J.; Petzold, C. J.; Kenttamaa, H. I. *J. Am. Chem. Soc.* **2002**, *124*, 12066.
(40) Kirk, B. B.; Harman, D. G.; Kenttämaa, H. I.; Trevitt, A. J.; Blanksby, S. J. *Phys. Chem. Chem. Phys.* **2012**, *14*, 16719.
(41) Kirk, B. B.; Harman, D. G.; Blanksby, S. J. *J. Phys. Chem. A* **2010**, *114*, 1446.
(42) Hansen, C. S.; Kirk, B. B.; Blanksby, S. J.; O'Hair, R. A. J.; Trevitt, A. J. *J. Am. Soc. Mass. Spectrom.* **2013**, *24*, 932.
(43) Ly, T.; Kirk, B. B.; Hettiarachchi, P. I.; Poad, B. L. J.; Trevitt, A. J.; da Silva, G.; Blanksby, S. J. *Phys. Chem. Chem. Phys.* **2011**, *13*, 16314.
(44) Frisch, M. J.; G. W. T., H. B. Schlegel, Scuseria, G. E.; Robb, M. A.; Cheeseman, J. R.; Scalmani, G.; Barone, V.; Mennucci, B.; Petersson, G. A.; Nakatsuji, H.; Caricato, M.; Li, X.; Hratchian, H. P.; Izmaylov, A. F.; Bloino, J.; Zheng, G.; Sonnenberg, J. L.; Hada, M.; Ehara, M.; Toyota, K.; Fukuda, R.; Hasegawa, J.; Ishida, M.; Nakajima, T.; Honda, Y.; Kitao, O.; Nakai, H.; Vreven, T.; Montgomery, J. A.; , Jr., Peralta, J. E.; Ogliaro, F.; Bearpark, M.; Heyd, J. J.; Brothers, E.; Kudin, K. N.; Staroverov, V. N.; Kobayashi, R.; Normand, J.; Raghavachari, K.; Rendell, A.; Burant, J. C.; Iyengar, S. S.; Tomasi, J.; Cossi, M.; Rega, N.; Millam, J. M.; Klene, M.; Knox, J. E.; Cross, J. B.; Bakken, V.; Adamo, C.; Jaramillo, J.; Gomperts, R.; Stratmann, R. E.; Yazyev, O.; Austin, A. J.; Cammi, R.; Pomelli, C.; Ochterski, J. W.; Martin, R. L.; Morokuma, K.; Zakrzewski, V. G.; Voth, G. A.; Salvador, P.; Dannenberg, J. J.; Dapprich, S.; Daniels, A. D.; Farkas, O.; Foresman, J. B.; Ortiz, J. V.; Cioslowski, J.; , and Fox, D. J. *Gaussian 09*, Revision A.02; Gaussian, Inc.: Wallingford, CT, 2009.
(45) Becke, A. D. *Phys. Rev. A* **1988**, *38*, 3098.
(46) Zhao, Y.; Truhlar, D. G. *Theor. Chem. Acc.* **2008**, *120*, 215.
(47) Cheng, P. Y.; Zhong, D.; Zewail, A. H. *Chem. Phys. Lett.* **1995**, *237*, 399.
(48) Harman, D. G.; Blanksby, S. J. *Org. Biomol. Chem.* **2007**, *5*, 3495.
(49) Bair, R. A.; Goddard, W. A. *J. Am. Chem. Soc.* **1982**, *104*, 2719.
(50) Zhao, Y.; Truhlar, D. G. *Acc. Chem. Res.* **2008**, *41*, 157.
(51) Jafri, J. A.; Phillips, D. H. *J. Am. Chem. Soc.* **1990**, *112*, 2586.
(52) Finlayson-Pitts, B. J.; Pitts, J. N., Jr. *Science* **1997**, *276*, 1045.
(53) Alfassi, Z. B.; Khaikin, G. I.; Neta, P. *J. Phys. Chem.* **1995**, *99*, 265.